AGU PUBLICATIONS

Water Resources Research

RESEARCH ARTICLE
10.1002/2016WR019101

Key Points:
- Analytical solutions of seawater intrusion in a sloping coastal aquifer
- Both confined and unconfined coastal aquifers are considered
- Both constant-flux and constant-head inland boundary conditions are examined

Correspondence to:
C. Lu,
clu@hhu.edu.cn

Citation:
Lu, C., P. Xin, J. Kong, L. Li, and J. Luo (2016), Analytical solutions of seawater intrusion in sloping confined and unconfined coastal aquifers, *Water Resour. Res.*, *52*, 6989–7004, doi:10.1002/2016WR019101.

Received 20 APR 2016
Accepted 27 AUG 2016
Accepted article online 1 SEP 2016
Published online 15 SEP 2016

Analytical solutions of seawater intrusion in sloping confined and unconfined coastal aquifers

Chunhui Lu[1], Pei Xin[1], Jun Kong[1], Ling Li[1,2], and Jian Luo[3]

[1]State Key Laboratory of Hydrology-Water Resources and Hydraulic Engineering, Hohai University, Nanjing, China, [2]School of Civil Engineering, University of Queensland, Brisbane, Queensland, Australia, [3]School of Civil and Environmental Engineering, Georgia Institute of Technology, Atlanta, Georgia, USA

Abstract Sloping coastal aquifers in reality are ubiquitous and well documented. Steady state sharp-interface analytical solutions for describing seawater intrusion in sloping confined and unconfined coastal aquifers are developed based on the Dupuit-Forchheimer approximation. Specifically, analytical solutions based on the constant-flux inland boundary condition are derived by solving the discharge equation for the interface zone with the continuity conditions of the head and flux applied at the interface between the freshwater zone and the interface zone. Analytical solutions for the constant-head inland boundary are then obtained by developing the relationship between the inland freshwater flux and hydraulic head and combining this relationship with the solutions of the constant-flux inland boundary. It is found that for the constant-flux inland boundary, the shape of the saltwater interface is independent of the geometry of the bottom confining layer for both aquifer types, despite that the geometry of the bottom confining layer determines the location of the interface tip. This is attributed to that the hydraulic head at the interface is identical to that of the coastal boundary, so the shape of the bed below the interface is irrelevant to the interface position. Moreover, developed analytical solutions with an empirical factor on the density factor are in good agreement with the results of variable-density flow numerical modeling. Analytical solutions developed in this study provide a powerful tool for assessment of seawater intrusion in sloping coastal aquifers as well as in coastal aquifers with a known freshwater flux but an arbitrary geometry of the bottom confining layer.

1. Introduction

The problem of seawater intrusion in coastal aquifers has increasingly become the main issue in managing freshwater resources in coastal regions and has attracted growing attention over recent decades [*Post and Abarca*, 2010; *Werner et al*., 2013]. The location of the interface between freshwater and seawater subject to various hydrologic and/or hydraulic stresses such as pumping and recharge is a key indicator for the sustainable management of coastal aquifers, reflecting the situation of aquifer salinization. Despite the availability of various numerical models [e.g., *Langevin and Guo*, 2006; *Bakker*, 2013], analytical solutions, as an effective first-order assessment tool, are frequently used to predict the steady state interface location.

Locating the freshwater-seawater interface requires solving simultaneously two coupled flow systems (i.e., flow in the freshwater zone and flow in the interface zone) in conjunction with the continuity conditions of the head and flux across the interface between the two zones. To facilitate the derivation of an analytical solution, a sharp interface is usually assumed, neglecting freshwater-seawater mixing. In other words, these two waters are considered immiscible. This assumption may be not appropriate for coastal aquifers where there is a thick mixing zone [e.g., *Lu et al*., 2009; *Lu and Luo*, 2010; *Lu et al*., 2013b]. Furthermore, analytical studies are typically based on the steady state condition assuming negligible hydrodynamic flow conditions caused by waves, tides, and seasonal variability in precipitation and groundwater extraction [e.g., *Ataie-Ashtiani et al*., 1999; *Xin et al*., 2010; *Kuan et al*., 2012].

Exact solutions have been developed for determining the sharp interface using the hodograph method in combination with conformal mapping [e.g., *Bear*, 1972; *Kacimov*, 2001; *Kacimov and Obnosov*, 2001; *Bakker*, 2014]. Moreover, sharp-interface analytical solutions have been derived based on the Ghyben-Herzberg relation [*Badon Ghyben and Drabbe*, 1888; *Herzberg*, 1901] together with the Dupuit-Forchheimer

approximation [*Dupuit*, 1863; *Forchheimer*, 1886] that neglects the flow in the vertical direction. *Strack* [1976], among others, presented an analytical technique for solving 3-D interface problems in a homogeneous coastal aquifer. This technique is based upon the use of a single potential throughout all zones (defined by the type of flow occurring) of an aquifer. *Pool and Carrera* [2011] introduced an empirical formula to take the mixing effect into account in the *Strack* potential by modifying the saltwater density according to the aquifer thickness and transverse dispersivity. *Beebe et al*. [2016] found that application of this empirical formula did not significantly improve the field results because of mismatches between simplifying assumptions of the analytical model and complex field settings. *Strack and Ausk* [2015] presented a comprehensive potential for interface flow in stratified aquifers, extending the applicability of the single-potential theory.

As a simple and pragmatic method, the single-potential approach has interested many researchers in solving interface flow problems under a verity of conditions [e.g., *Park et al*., 2009; *Lu et al*., 2015]. For example, this approach has been employed to develop effective pumping well optimization strategies in coastal aquifers subject to seawater intrusion problems [e.g., *Cheng et al*., 2000; *Mantoglou*, 2003; *Lu et al*., 2013c], to explore the vulnerability of coastal aquifers to groundwater use and sea-level rise [*Ferguson and Gleeson*, 2012; *Lu et al*., 2013a], and to examine the impact of the boundary condition and aquifer size on the maximum pumping rate in a coastal aquifer [*Lu et al*., 2012; *Lu and Luo*, 2014].

Relying on the single-potential approach, *Koussis et al*. [2012] developed analytical solutions for regional seawater intrusion in sloping unconfined coastal aquifers with uniform recharge and a line sink. The discharge potential of the interface zone shares the same form as that of *Strack* [1976] for the case of a horizontal aquifer, but with a different constant. The flow potential of the upgradient side of the interface tip (i.e., the freshwater zone) is obtained through the approximation of a linearized hydraulic potential due to gravity. *Mazi et al*. [2013] applied the analytical solution of *Koussis et al*. [2012] to evaluate the impact of sea-level rise on seawater intrusion in both flux-controlled and head-controlled sloping unconfined coastal aquifers. Moreover, *Mazi et al*. [2013] adopted the analytical solution of *Koussis et al*. [2012] to investigate seawater intrusion in three major Mediterranean aquifers. More recently, *Koussis et al*. [2015] introduced a correction to their analytical solutions to account for the submarine outflow gap. In addition to analytical studies, the numerical approach has been taken to study seawater intrusion in an unconfined sloping aquifer [e.g., *Qahman and Zhou*, 2001; *Abarca et al*., 2002].

In fact, the topic of flow in a sloping aquifer has long been investigated [e.g., *Henderson and Wooding*, 1964; *Huang et al*., 2014]. Steady state solutions of the nonlinear Boussinesq equation for homogeneous unconfined flow in sloping aquifers with recharge have been derived analytically by *McEnroe* [1993], *Verhoest and Troch* [2000], *Chapuis* [2002], and *Loáiciga* [2005]. The latter three solutions have been reviewed and compared by *Chapuis* [2011]. It is found that the two solutions developed by *Chapuis* [2002] and *Loáiciga* [2005] are essentially the same, both based on the Dupuit-Forchheimer approximation. Based on the linearized Boussinesq equation, various analytical solutions have been developed for transient unconfined flow in sloping aquifers with recharge [e.g., *Basha and Maalouf*, 2005; *Akylas et al*., 2006].

This study aims to develop steady state sharp-interface analytical solutions for seawater intrusion in sloping coastal aquifers. Examples of sloping coastal aquifers in reality are numerous [e.g., *Sherif and Singh*, 1999; *Koussis et al*., 2010]. Different from the single-potential method used in *Koussis et al*. [2012], analytical solutions will be developed by solving the discharge equation for the interface zone and applying the continuity conditions of the head and flux at the interface between the freshwater zone and the interface zone. Although unconfined sloping aquifers have been investigated, analytical solutions for seawater intrusion in confined sloping aquifers are not available, to the best of our knowledge, and will also be derived in this study. For both types of aquifers, constant-head and constant-flux inland boundary conditions will be considered. The importance of the inland boundary condition on seawater intrusion has been highlighted by a number of studies [*Werner and Simmons*, 2009; *Lu et al*., 2012; *Mazi et al*., 2013; *Lu et al*., 2015]. Hypothetical examples will be used to demonstrate the application of the new analytical solutions.

2. Conceptual Model

We consider both confined and unconfined sloping coastal aquifers, which are idealized and simplified. For both aquifer types, the following assumptions are made in deriving the analytical solutions: (1) flow systems are under

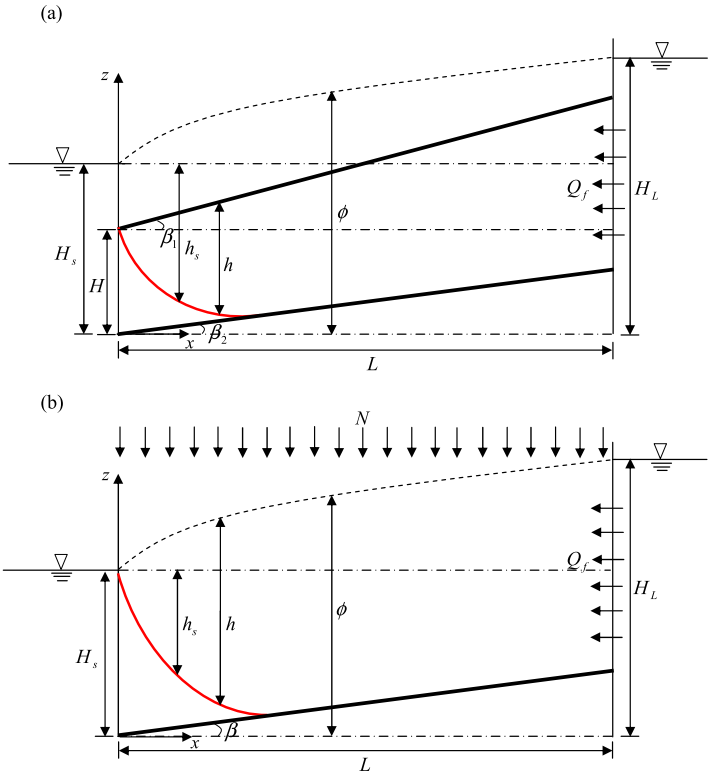

Figure 1. Conceptual models of a (a) confined and (b) unconfined sloping coastal aquifer.

steady state; (2) the interface between freshwater and seawater is sharp; (3) the aquifer is hydraulically homogeneous and isotropic; and (4) the flow in the vertical direction is neglected (i.e., the Dupuit-Forchheimer approximation is adopted).

Figure 1 shows the conceptual models of a sloping confined and a sloping unconfined coastal aquifer. For both conceptual models, the origin of the coordinate system is located at the intersection of the coastal boundary and the bottom confining layer. Specifically, the z axis is vertically upward, while the x axis is pointing horizontally landward. The datum of the aquifer system is at the same level as the x-axis. The elevation of the sea level is H_s. The freshwater flux flowing from inland to the sea is Q_f (negative). The hydraulic head at the distance L from the coastline is H_L. When deriving the analytical solution, we apply only one inland boundary condition (i.e., either Q_f or H_L), i.e., solutions will be derived respectively for the constant-head and the constant-flux inland boundary condition. The vertical thickness of the layer between the sea level and the interface is h_s, while the vertical thickness of the freshwater lens is h. φ is the hydraulic head above the datum (i.e. the x axis). For the unconfined aquifer, a uniform recharge (N) is considered along the entire aquifer surface.

For the confined coastal aquifer, both the top and bottom confining layers may be inclined, with angles of $\beta_1$and β_2, respectively. The vertical thickness of the confined aquifer at the coastal boundary is H. For the unconfined coastal aquifer, the bottom confining layer is assumed inclined, with an angle of β.

3. Derivation of Analytical Solutions

In the following, we derive analytical solutions for both confined and unconfined coastal aquifers. For each type of aquifer, a constant-flux and a constant-head inland boundary condition will be adopted, respectively.

3.1 Confined Aquifer With A Constant-Flux Inland Boundary Condition

Based on the Dupuit-Forchheimer approximation, the freshwater discharge is calculated by:

$$Q_f = -Kh\frac{d\varphi}{dx} \tag{1}$$

Applying the Ghyben-Herzberg relation, the vertical thickness of the freshwater lens (h) in the interface zone can be written as (see Appendix A):

$$h = \alpha(\varphi - H_s) - [H_s - H - x\tan(\beta_1)] \tag{2}$$

in which α is the density ratio defined as the freshwater density relative to the density difference between seawater and freshwater. Taking the first-order derivative with respect to x on both sides of equation (2) yields:

$$\frac{dh}{dx}=\alpha\frac{d\varphi}{dx}+\tan(\beta_1) \tag{3}$$

Combining equations (1) and (3) gives:

$$\frac{dh}{dx}=\alpha\left(-\frac{Q_f}{Kh}\right)+\tan(\beta_1) \tag{4}$$

Equation (4) can be written as:

$$\frac{dh}{\left[-\alpha\frac{Q_f}{Kh}+\tan(\beta_1)\right]}=dx \tag{5}$$

The derivation of the solution of equation (5) depends on the condition whether the value of β_1 is equal to zero.

If $\beta_1=0$, equation (5) is simplified as:

$$\frac{Khdh}{-\alpha Q_f}=dx \tag{6}$$

The solution of equation (6) is given by:

$$\frac{K}{-\alpha Q_f}\frac{h^2}{2}=x+C_1 \tag{7}$$

in which C_1 is an integration constant, and can be determined by the coastal boundary condition:

$$x=0,\quad h=0, \tag{8}$$

Thus, $C_1=0$ and equation (7) is then expressed as:

$$x=\frac{K}{-\alpha Q_f}\frac{h^2}{2} \tag{9}$$

Equation (9) can be used to determine the interface location. At the interface tip, the relationship between the vertical thickness of the freshwater lens (h_t) and the x-coordinate (x_t) is given by:

$$h_t=H-x_t\tan(\beta_2) \tag{10}$$

Replacing x and h in equation (9) by x_t and h_t, respectively, and substitution of equations (10) into (9) yield:

$$x_t=\frac{K}{-\alpha Q_f}\frac{[H-x_t\tan(\beta_2)]^2}{2} \tag{11}$$

If $\beta_2=0$, the confined aquifer is horizontal with a constant thickness. The location of the interface tip determined by equation (11) is exactly the same as the solution derived previously by the single-potential method [*Strack*, 1989; *Lu et al.*, 2015]. If $\beta_2\neq 0$, rearrangement of equation (11) gives:

$$K\tan^2(\beta_2)x_t^2+(2\alpha Q_f-2HK\tan(\beta_2))x_t+KH^2=0 \tag{12}$$

The solution of equation (12) is derived as:

$$x_t=\frac{-(\alpha Q_f-HK\tan(\beta_2))-\sqrt{\alpha^2Q_f^2-2HK\alpha Q_f\tan(\beta_2)}}{\tan^2(\beta_2)K} \tag{13}$$

Note that the other solution to equation (12) with the positive square root term is not physically meaningful, since x_t increases with decreasing freshwater influx (i.e., $-Q_f$) but with increasing H and K. It is obvious that when $\beta_1=0$, the solution of x_t is continuous at $\beta_2=0$. A maximum value of x_t occurs, when $\alpha^2Q_f^2-2HK\alpha Q_f\tan(\beta_2)=0$. Because Q_f is negative, $\tan(\beta_2)$ must be negative such that the maximum interface tip location ($x_t^{\max}$) exists:

$$x_t^{\max}=-\frac{H}{\tan(\beta_2)} \tag{14}$$

It is shown that $x_t^{\max}$ is only a function of H and β_2. Furthermore, since x_t is a real number, $\alpha^2Q_f^2-2HK\alpha Q_f\tan(\beta_2)\geq 0$, which leads to $Q_f\leq\frac{2HK\tan(\beta_2)}{\alpha}$. Q_f is always less than $\frac{2HK\tan(\beta_2)}{\alpha}$, if $\tan(\beta_2)\geq 0$.

However, if $\tan(\beta_2) < 0$ and $Q_f > \frac{2HK\tan(\beta_2)}{\alpha}$, no solution of x_t exists because there is no intersection between the interface and the bottom confining layer, i.e., the absolute gradient of the interface above the bottom confining layer is less than that of the bottom confining layer.

If $\beta_1 \neq 0$, equation (5) can be rearranged as:

$$\left[1+\frac{\alpha Q_f}{-\alpha Q_f + Kh\tan(\beta_1)}\right]dh = \tan(\beta_1)dx \tag{15}$$

Integrating both sides of the equation gives:

$$h+\frac{\alpha Q_f}{K\tan(\beta_1)}\ln\left[-\alpha Q_f + Kh\tan(\beta_1)\right] = x\tan(\beta_1)+C_2 \tag{16}$$

in which C_2 is an integration constant and can be determined by the coastal boundary condition (i.e., equation (8)):

$$C_2 = \frac{\alpha Q_f}{K\tan(\beta_1)}\ln\left[-\alpha Q_f\right] \tag{17}$$

Thus, substitution of equation (17) into (16) generates:

$$h+\frac{\alpha Q_f}{K\tan(\beta_1)}\ln\left[1+\frac{Kh\tan(\beta_1)}{-\alpha Q_f}\right] = x\tan(\beta_1) \tag{18}$$

Equation (18) can be employed to determine the interface location. At the interface tip, the relationship between h_t and x_t is given by:

$$h_t = H - x_t\tan(\beta_2) + x_t\tan(\beta_1) \tag{19}$$

Replacing x and h in equation (18) by x_t and $h_t$and inserting equation (19) into (18) yield:

$$H - x_t\tan(\beta_2)+\frac{\alpha Q_f}{K\tan(\beta_1)}\ln\left[1+\frac{K\tan(\beta_1)(H - x_t\tan(\beta_2)+x_t\tan(\beta_1))}{-\alpha Q_f}\right] = 0 \tag{20}$$

x_t can be determined based on equation (20) using the Newton-Raphson method.

The analytical solutions for seawater intrusion in confined aquifers with a constant-flux boundary condition and various conditions of β_1 and β_2 are listed in Table 1.

3.2. Confined Aquifer With A Constant-Head Inland Boundary Condition

Alternatively, the hydraulic head at a distance of L from the coastline (i.e.,H_L) may be available, while the freshwater flux from inland (i.e.,Q_f) is unknown. The analytical solution for the constant-head inland boundary condition can be developed by deriving the relationship between the inland freshwater flux and hydraulic head and using the analytical solution of the constant-flux boundary condition.

Based on the Dupuit-Forchheimer approximation, the freshwater discharge in the aquifer section between the inland boundary and the interface tip (i.e., the freshwater zone) follows:

$$Q_f = -K(H+(\tan(\beta_1)-\tan(\beta_2))x)\frac{d\varphi}{dx} \tag{21}$$

If $\beta_1 = \beta_2$, equation (21) is simplified as:

$$Q_f = -KH\frac{d\varphi}{dx} \tag{22}$$

Integrating equation (22) yields:

$$\varphi = -\frac{Q_f}{KH}x + C_3 \tag{23}$$

The integration constant C_3 can be determined using the inland boundary condition (i.e., $x = L$, $\varphi = H_L$):

Table 1. Analytical Solutions of Seawater Intrusion in Confined Aquifers With a Constant-Flux Boundary Condition

β_1	β_2	Interface Tip Location	Interface Location
0	0	$x_t=\frac{KH^2}{-2\alpha Q_f}$	$x=\frac{K}{-\alpha Q_f}\frac{h^2}{2}$
	$\neq 0$	$x_t=\frac{-(\alpha Q_f-HK\tan(\beta_2))-\sqrt{\alpha^2Q_f^2-2HK\alpha Q_f\tan(\beta_2)}}{\tan^2(\beta_2)K}$	
$\neq 0$	0	$H-x_t\tan(\beta_2)+\frac{\alpha Q_f}{K\tan(\beta_1)}\ln\left[1+\frac{K\tan(\beta_1)(H-x_t\tan(\beta_2)+x_t\tan(\beta_1))}{-\alpha Q_f}\right]=0$	$h+\frac{\alpha Q_f}{K\tan(\beta_1)}\ln\left[1+\frac{K h\tan(\beta_1)}{-\alpha Q_f}\right]=x\tan(\beta_1)$
	$\neq 0$		

$$C_3=\frac{Q_f}{KH}L+H_L \tag{24}$$

Equation (23) is then expressed as:

$$\varphi=-\frac{Q_f}{KH}(x-L)+H_L \tag{25}$$

At the interface tip, we have:

$$x=x_t,\ \ \varphi=\varphi_t=\frac{1+\alpha}{\alpha}(H_s-x_t\tan(\beta_2))+x_t\tan(\beta_2) \tag{26}$$

Substitution of equation (26) into (25) yields:

$$\frac{1+\alpha}{\alpha}(H_s-x_t\tan(\beta_2))+x_t\tan(\beta_2)=-\frac{Q_f}{KH}(x_t-L)+H_L \tag{27}$$

Thus, Q_f can be expressed as:

$$Q_f=-\frac{KH}{(x_t-L)}\left[\frac{1+\alpha}{\alpha}(H_s-x_t\tan(\beta_2))+x_t\tan(\beta_2)-H_L\right] \tag{28}$$

If $\beta_1\neq\beta_2$, equation (21) can be integrated as:

$$\varphi=-\frac{Q_f}{K(\tan(\beta_1)-\tan(\beta_2))}\ln\left[H+(\tan(\beta_1)-\tan(\beta_2))x\right]+C_4 \tag{29}$$

The integration constant C_4 can be determined using the inland boundary condition:

$$C_4=\frac{Q_f}{K(\tan(\beta_1)-\tan(\beta_2))}\ln\left[H+(\tan(\beta_1)-\tan(\beta_2))L\right]+H_L \tag{30}$$

Thus, equation (29) is expressed as:

$$\varphi=-\frac{Q_f}{K(\tan(\beta_1)-\tan(\beta_2))}\ln\left[\frac{H+(\tan(\beta_1)-\tan(\beta_2))x}{H+(\tan(\beta_1)-\tan(\beta_2))L}\right]+H_L \tag{31}$$

The validity of equation (31) requires the logarithm of a positive real number, resulting in that $L<-\frac{H}{(\tan(\beta_1)-\tan(\beta_2))}$ when $\tan(\beta_1)-\tan(\beta_2)<0$. Applying the boundary condition at the interface tip and substituting equation (26) into (31) yield:

$$\frac{1+\alpha}{\alpha}(H_s-x_t\tan(\beta_2))+x_t\tan(\beta_2)=-\frac{Q_f}{K(\tan(\beta_1)-\tan(\beta_2))}\ln\left[\frac{H+(\tan(\beta_1)-\tan(\beta_2))x_t}{H+(\tan(\beta_1)-\tan(\beta_2))L}\right]+H_L \tag{32}$$

Rearrangement of equation (32) gives:

$$Q_f=\frac{-K(\tan(\beta_1)-\tan(\beta_2))\left[\frac{1+\alpha}{\alpha}H_s-\frac{\tan(\beta_2)}{\alpha}x_t-H_L\right]}{\ln\left[\frac{H+(\tan(\beta_1)-\tan(\beta_2))x_t}{H+(\tan(\beta_1)-\tan(\beta_2))L}\right]} \tag{33}$$

Equation (28) or (33) can be used in conjunction with the solution of the constant-flux inland boundary condition (i.e., equation (13) or (20)) to determine x_t and Q_f for the constant-head inland boundary condition using the trial-and-error method. Subsequently, the interface location can be derived using equation (9) or (18).

3.3. Unconfined Aquifer With A Constant-Flux Inland Boundary Condition

Similarly, the freshwater discharge can be determined for the unconfined aquifer based on the Dupuit-Forchheimer approximation:

$$Q_f-(L-x)N=-Kh\frac{d\varphi}{dx} \tag{34}$$

For the interface zone, the relation between h and φ is given by the Ghyben-Herzberg relation:

$$h=(1+\alpha)(\varphi-H_s) \tag{35}$$

Inserting equation (35) into (34) and integrating the equation give:

$$Q_f x-NLx+N\frac{x^2}{2}+C_5=-(1+\alpha)K\frac{(\varphi-H_s)^2}{2} \tag{36}$$

in which C_5 is the integration constant and equal to zero, determined by the coastal boundary condition (i.e., $x=0$, $\varphi=H_s$). The relation between φ and h_s is given by:

$$h_s=\alpha(\varphi-H_s) \tag{37}$$

Combining equations (36) and (37) and eliminating φ produce:

$$Q_f x-NLx+N\frac{x^2}{2}=-(1+\alpha)K\frac{h_s^2}{2\alpha^2} \tag{38}$$

Equation (38) can be applied to determine the interface toe location. As indicated, the shape of the interface is independent of the geometry of the aquifer bed. The reason for this phenomenon is that the hydraulic head at the interface is determined by the coastal boundary, so the shape of the bed below the interface is in no relation to the interface position. At the interface tip, we have:

$$x=x_t,\quad \varphi=\varphi_t=\frac{1+\alpha}{\alpha}(H_s-x_t\tan(\beta))+x_t\tan(\beta) \tag{39}$$

The location of the interface tip is obtained by inserting equation (39) into (36):

$$Q_f x_t-NLx_t+N\frac{x_t^2}{2}=-(1+\alpha)K\frac{\left(\frac{1}{\alpha}(H_s-x_t\tan(\beta))\right)^2}{2} \tag{40}$$

Rearrangement of equation (40) yields:

$$\left(N+\frac{(1+\alpha)}{\alpha^2}K\tan^2(\beta)\right)x_t^2+2\left(Q_f-NL-\frac{(1+\alpha)}{\alpha^2}KH_s\tan(\beta)\right)x_t+\frac{(1+\alpha)}{\alpha^2}KH_s^2=0 \tag{41}$$

Equation (40) is essentially the same as equation ((26)b) in *Koussis et al.* [2012]. Note that the x axis in *Koussis et al.* [2012] is along the aquifer bed. In addition, *Koussis et al.* [2012] considered an additional term of a line sink in their equation. The line sink can be readily included in our conceptual model as well as in the equation above. To solve equation (41), we let:

$$a=N+\frac{(1+\alpha)}{\alpha^2}K\tan^2(\beta) \tag{42a}$$

$$b=2\left(Q_f-NL-\frac{(1+\alpha)}{\alpha^2}KH_s\tan(\beta)\right) \tag{42b}$$

$$c=\frac{(1+\alpha)}{\alpha^2}KH_s^2 \tag{42c}$$

If $a=0$, N and $\tan(\beta)$ must equal to zero. The simplified case is exactly the same as that in *Strack* [1976]. Under such a scenario, the solution is given by:

$$x_t=-\frac{(1+\alpha)}{\alpha^2}\frac{KH_s^2}{2Q_f} \tag{43}$$

Equation (43) is exactly the same as that previously developed by *Strack* [1976].

If $a \neq 0$, the solutions of equation (41) are expressed by:

$$x_t = \frac{-b \pm \sqrt{b^2 - 4ac}}{2a} \tag{44}$$

The existence of real roots requires that $b^2 - 4ac \geq 0$. As indicated by *Koussis et al*. [2012], only the negative square root term is physically meaningful, since x_t increases with increasing H_s and K but with decreasing $-Q_f$ and N. Moreover, a maximum value of x_t occurs when $b^2 - 4ac = 0$:

$$x_t^{\max} = \frac{H_s}{\alpha}[(1+\alpha)K]^{1/2}\left[N + \frac{(1+\alpha)}{\alpha^2}K\tan^2(\beta)\right]^{-1/2} \tag{45}$$

Equation (45) is essentially the same as equation (28) in *Koussis et al*. [2012]. If we assume $N = 0$, $b^2 - 4ac = 4Q_f^2 - 8\frac{(1+\alpha)}{\alpha^2}KH_sQ_f\tan(\beta)$. Since Q_f is negative, $\tan(\beta)$ must be negative such that $b^2 - 4ac$ can be equal to zero. Then, equation (45) is simplified to:

$$x_t^{\max} = -\frac{H_s}{\tan(\beta)} \tag{46}$$

Equation (46) is similar to equation (14). The difference between two equations is that the numerator in equation (14) is H, while in equation (46) it is H_s.

3.4. Unconfined Aquifer With A Constant-Head Inland Boundary Condition

To develop analytical solutions for the unconfined sloping aquifer with a constant-head inland boundary condition, again one only needs to derive the relationship between the inland hydraulic head and freshwater discharge, given the availability of the solutions for the constant-flux inland boundary condition. The freshwater discharge is given by equation (34). For the aquifer between the inland boundary and the interface tip, h is expressed by:

$$h = \varphi - x\tan(\beta) \tag{47}$$

Taking the first-order derivative of h with respect to x:

$$\frac{dh}{dx} = \frac{d\varphi}{dx} - \tan(\beta) \tag{48}$$

Substitution of equation (48) into (34) gives:

$$h\frac{dh}{dx} + h\tan(\beta) + \frac{Q_f - N(L-x)}{K} = 0 \tag{49}$$

The solution of equation (49) depends on whether N is zero or not. If $N = 0$, equation (49) can be simplified as:

$$h\frac{dh}{dx} + h\tan(\beta) + \frac{Q_f}{K} = 0 \tag{50}$$

If $\beta = 0$, the confining bed is horizontal, and the interface tip location has been derived by *Lu et al*. [2015]:

$$x_t = \frac{(1+\alpha)LH_s^2}{\alpha^2 H_L^2 - (1+\alpha)\alpha H_s^2} \tag{51}$$

The solution of equation (50) for the condition of $\beta \neq 0$ is expressed by:

$$h - \frac{Q_f}{K\tan(\beta)}\ln[-Kh\tan(\beta) - Q_f] = -x\tan(\beta) + C_6 \tag{52}$$

The integration constant C_6 can be determined using the inland boundary condition (i.e., $x = L$, $h = H_L - L\tan(\beta)$):

$$C_6 = H_L - \frac{Q_f}{K\tan(\beta)}\ln[-K(H_L - L\tan(\beta))\tan(\beta) - Q_f] \tag{53}$$

Thus, equation (52) is expressed as:

$$h=-x\tan(\beta)+H_L+\frac{Q_f}{K\tan(\beta)}\ln\left[\frac{-Kh\tan(\beta)-Q_f}{-K(H_L-L\tan(\beta))\tan(\beta)-Q_f}\right] \tag{54}$$

Applying the boundary condition at the interface tip (i.e., $x=x_t$, $h=\varphi_t-x_t\tan(\beta)$) to equation (54) gives:

$$\varphi_t=H_L+\frac{Q_f}{K\tan(\beta)}\ln\left[\frac{-K(\varphi_t-x_t\tan(\beta))\tan(\beta)-Q_f}{-K(H_L-L\tan(\beta))\tan(\beta)-Q_f}\right] \tag{55}$$

in which $\varphi_t=\frac{1+\alpha}{\alpha}(H_s-x_t\tan(\beta))+x_t\tan(\beta)$. Equation (55) is an implicit equation for Q_f, while Q_f in equation (40) can be explicitly expressed. Thus, Q_f in equation (55) can be replaced by the analytical expression based on equation (40), resulting in an equation that only involves an unknown parameter of x_t. Then, x_t can be determined numerically using the Newton-Raphson method. Moreover, the validity of equation (55) requires that $L>\frac{H_L}{\tan(\beta)}+\frac{Q_f}{K\tan^2(\beta)}$ if $\tan(\beta)>0$.

The steady state analytical solution for groundwater flow in a sloping unconfined aquifer recharged by a uniform infiltration has been developed independently by *Chapuis* [2002] and *Loáiciga* [2005]. The method used here is similar to that employed by *Chapuis* [2002]. If $N\neq 0$, we let:

$$Y=h \tag{56}$$

$$X=\frac{(Q_f-N(L-x))}{K}\sqrt{\frac{K}{N}} \tag{57}$$

Equation (49) can be rewritten as:

$$Y\frac{dY}{dX}+rY+X=0 \tag{58}$$

in which $r=\tan(\beta)\sqrt{\frac{K}{N}}$. It has been shown that the solution of equation (58) depends on the absolute value of r [*Chapuis*, 2002; *Loáiciga*, 2005]:

$$\begin{cases}(X\pm Y)e^{\frac{X}{X\pm Y}}=C_7, & |r|=2\\ \ln|Y^2+rXY+X^2|-\dfrac{2r}{\sqrt{4-r^2}}\arctan\left(\dfrac{2Y+rX}{X\sqrt{4-r^2}}\right)=C_7, & |r|<2\\ |Y-\lambda X|^{\lambda}=C_7|Y-\mu X|^{\mu}, & |r|>2\end{cases} \tag{59}$$

in which C_7 is a constant, and λ and μ are expressed as:

$$\lambda,\mu=-\frac{r}{2}\pm\frac{\sqrt{r^2-4}}{2} \tag{60}$$

The constant C_7 can be obtained based on the boundary condition at the interface tip (i.e., $X_t=\frac{(Q_f-N(L-x_t))}{K}\sqrt{\frac{K}{N}}$, $Y_t=\frac{1+\alpha}{\alpha}(H_s-x_t\tan(\beta))$):

$$\begin{cases}C_7=(X_t\pm Y_t)e^{\frac{X_t}{X_t\pm Y_t}}, & |r|=2\\ C_7=\ln|Y_t^2+rX_tY_t+X_t^2|-\dfrac{2r}{\sqrt{4-r^2}}\arctan\left(\dfrac{2Y_t+rX_t}{X_t\sqrt{4-r^2}}\right), & |r|<2\\ C_7=\dfrac{|Y_t-\lambda X_t|^{\lambda}}{|Y_t-\mu X_t|^{\mu}}, & |r|>2\end{cases} \tag{61}$$

Thus, equation (59) becomes:

$$\begin{cases}(X\pm Y)e^{\frac{X}{X\pm Y}}-(X_t\pm Y_t)e^{\frac{X_t}{X_t\pm Y_t}}=0, & |r|=2\\ \ln\left[\dfrac{|Y^2+rXY+X^2|}{|Y_t^2+rX_tY_t+X_t^2|}\right]-\dfrac{2r}{\sqrt{4-r^2}}\left[\arctan\left(\dfrac{2Y+rX}{X\sqrt{4-r^2}}\right)-\arctan\left(\dfrac{2Y_t+rX_t}{X_t\sqrt{4-r^2}}\right)\right]=0, & |r|<2\\ |Y-\lambda X|^{\lambda}|Y_t-\mu X_t|^{\mu}-|Y_t-\lambda X_t|^{\lambda}|Y-\mu X|^{\mu}=0, & |r|>2\end{cases} \tag{62}$$

In addition, we have the following inland boundary condition:

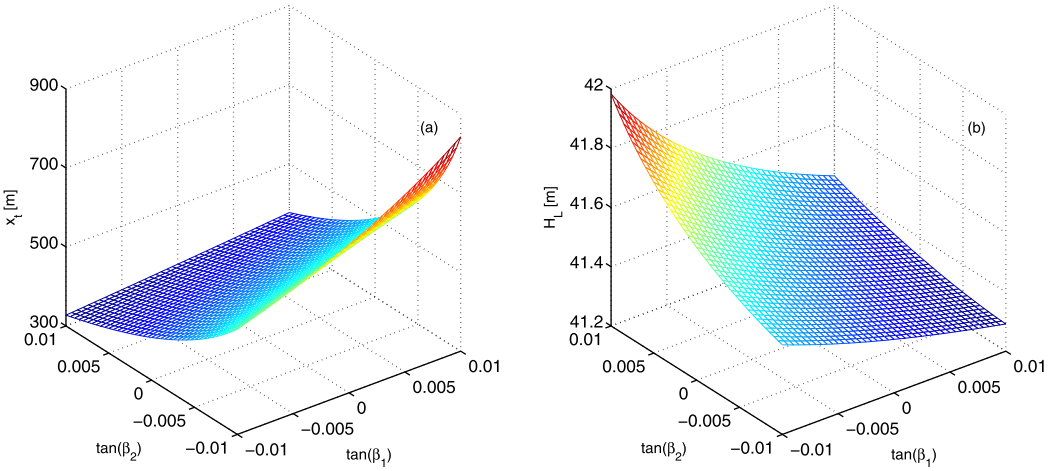

Figure 2. (a) Interface tip locations and (b) inland hydraulic heads in a confined aquifer with a constant-flux inland boundary condition ($Q_f = -0.3$ m^2/d) for different combinations of tan (β_1) and tan (β_2) between -0.01 and 0.01.

$$X_L = \frac{Q_f}{\sqrt{KN}}, \quad Y_L = H_L - L\tan\beta, \tag{63}$$

Then, the interface tip location can be derived based on the equation below:

$$\begin{cases} (X_L \pm Y_L)e^{\frac{X_L}{X_L \pm Y_L}} - (X_t \pm Y_t)e^{\frac{X_t}{X_t \pm Y_t}} = 0, & |r| = 2 \\ \ln\left[\dfrac{|Y_L{}^2 + rX_LY_L + X_L{}^2|}{|Y_t{}^2 + rX_tY_t + X_t{}^2|}\right] - \dfrac{2r}{\sqrt{4-r^2}}\left[\arctan\left(\dfrac{2Y_L + rX_L}{X_L\sqrt{4-r^2}}\right) - \arctan\left(\dfrac{2Y_t + rX_t}{X_t\sqrt{4-r^2}}\right)\right] = 0, & |r| < 2 \\ |Y_L - \lambda X_L|^{\lambda}|Y_t - \mu X_t|^{\mu} - |Y_t - \lambda X_t|^{\lambda}|Y_L - \mu X_L|^{\mu} = 0, & |r| > 2 \end{cases} \tag{64}$$

Since the equations presented here are for the constant-head inland boundary condition, $Q_f$and x_t are unknown. The two parameters can be solved by combing equations (44) and (64) using the standard methods for nonlinear equations.

3.5. Correction Factor

Analytical solutions derived above are based on the assumption of the sharp interface. In other words, the dispersive mixing between freshwater and seawater is neglected. This assumption usually leads to a significant difference between analytical solutions and corresponding variable-density flow numerical solutions. To overcome this issue, *Pool and Carrera* [2011] introduced an empirical factor on the density factor:

$$\alpha\prime = \alpha\left[1 - \left(\frac{\alpha_T}{B}\right)^{1/6}\right]^{-1} \tag{65}$$

in which α_T is the transverse dispersivity, and B is the aquifer thickness. Later, *Lu and Werner* [2013] found that the exponential of 1/6 should be replaced by 1/4 for better locating the interface toe. As such, we modify equation (65) as:

$$\alpha\prime = \alpha\left[1 - \left(\frac{\alpha_T}{B}\right)^{1/4}\right]^{-1} \tag{66}$$

Since the thickness of the sloping aquifers is nonuniform, we assume that $B=H$ for confined aquifers and $B=H_s$ for unconfined aquifers. We select the aquifer thickness at the coastal boundary instead of the mean aquifer thickness, because the shape of the interface is not controlled bytan (β_2) for a flux-controlled coastal system, as shown by the solutions above.

4. Examples

4.1. Confined Aquifers

We first consider confined aquifers with a constant-flux inland boundary condition. The two confining beds may be inclined. The data are given below.

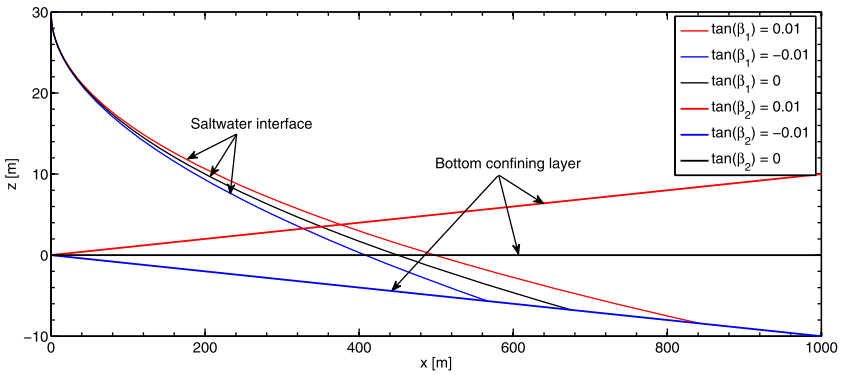

Figure 3. Interface toes (solid lines) and bottom aquifer beds (dashed lines) fortan $(\beta_1) = -0.01$, 0, and 0.01, and tan $(\beta_2) = -0.01$, 0, and 0.01.

$$H=30m,\ K=10m/d,\ \alpha=40,\ Q_f=-0.3m^2/d,\ H_s=40m, \tag{67}$$

In addition, we assume that tan (β_1) and tan $(\beta_2)$are varied between -0.01 and 0.01, corresponding to anglesβ_1 and β_2 between $-0.57°$ and 0.57°, respectively.

Figure 2 shows the interface tip locations and corresponding inland hydraulic heads at $L = 1000$ m for confined aquifer cases with a constant-flux inland boundary condition for different combinations of tan (β_1) and tan (β_2). It is shown that x_t is varied between 327.4 and 842.7 m, and a larger tan (β_1) and a smaller tan (β_2) result in a larger x_t. By contrast, H_L at $L = 1000$ m is between 41.29 and 41.98 m, and a smaller tan (β_1) and a higher tan (β_2) yield a higher H_L.

Figure 3 shows the saltwater interfaces (fine lines) and bottom confining layers (coarse lines) for tan $(\beta_1) = -0.01$, 0, and 0.01, and tan $(\beta_2) = -0.01$, 0, and 0.01. Given a value oftan (β_1), the interfaces for different values of tan (β_2)overlap for the upper section, while tan (β_2) controls the interface tip location, as suggested by equations (18) and (20). In comparison to a horizontal upper confining layer, a positive value of tan (β_1)leads to a more inland interface and a negative value a more seaward interface. Moreover, a smallertan (β_2)results in a larger difference of x_t between cases with differenttan (β_1), which is consistent with the finding in Figure 2.

Then, a constant-head inland boundary condition at $L = 1000$ m is fixed with $H_L = 41.6$ m. Figure 4 shows the interface tip locations and corresponding inland freshwater fluxes for different combinations of tan (β_1) andtan (β_2). x_t is between 321.5 and 490.9 m and a smaller tan (β_1) and tan (β_2) lead to a larger x_t, while the magnitude of the inland freshwater flux (i.e., $-Q_f$) is between 0.18 and 0.38 m^2/d, increasing with a larger tan (β_1) and a smaller tan (β_2).

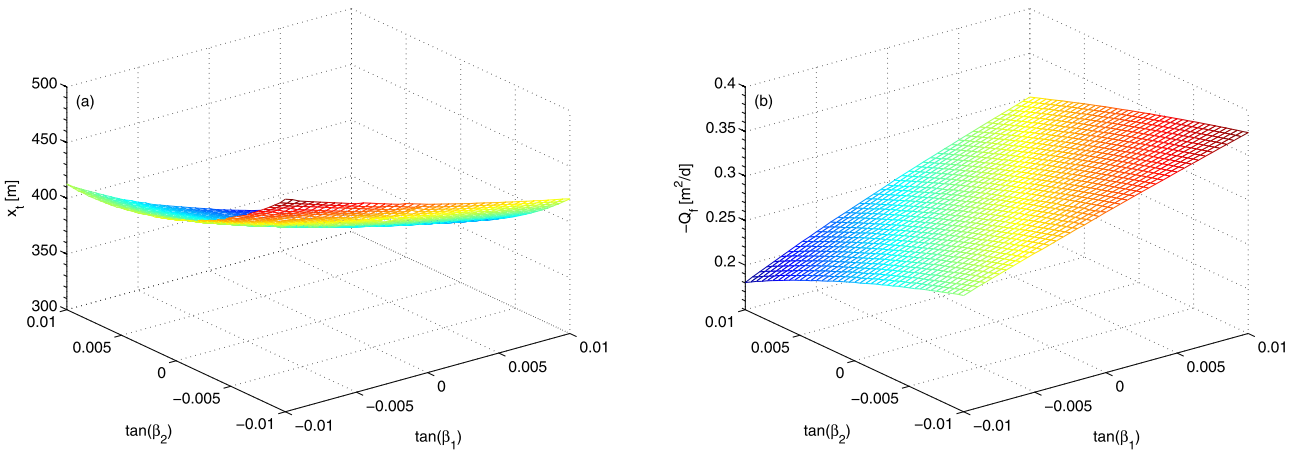

Figure 4. (a) Interface tip locations and (b) the inland freshwater fluxes in a confined aquifer with a constant-head inland boundary condition ($H_L = 41.6$ m) for different combinations of tan (β_1) and tan (β_2) between -0.01 and 0.01.

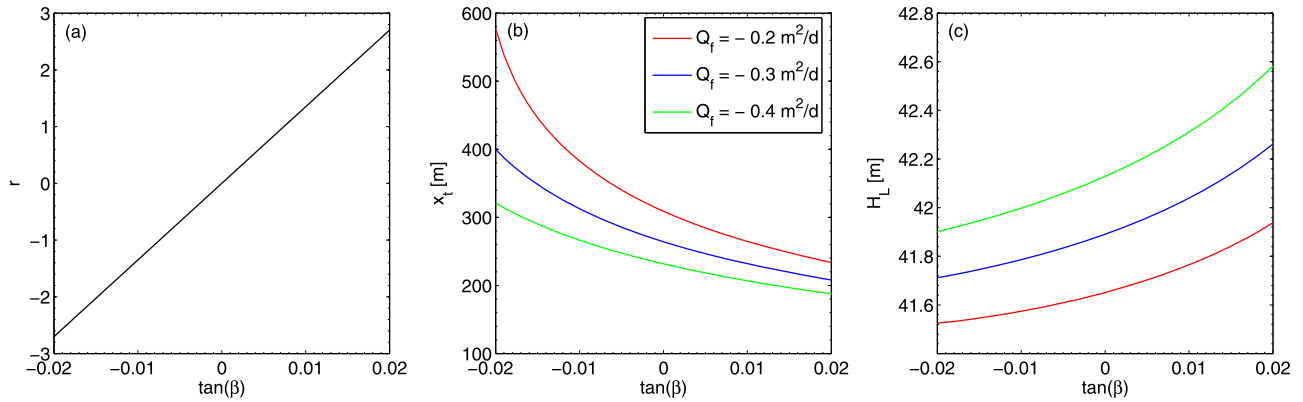

Figure 5. Values of (a) r, (b) x_t, and (c) H_L for different values of tan(β) and $Q_f = -0.2$, -0.3, and -0.4 m^2/d.

4.2. Unconfined Aquifers

Unconfined aquifers are considered with the following data:

$$H_s = 40m,\ K = 10m/d,\ \alpha = 40,\ N = 200mm/yr,\ L = 1000m, \tag{68}$$

Here, we assume that tan (β) varies between -0.02 and 0.02 (corresponding to angles between $-1.15°$ and 1.15°) such that $|r|$ can be larger, equal to, or less than 2.

Figure 5 shows the values of r, interface tip locations, and inland hydraulic heads for different tan (β) and $Q_f = -0.2$, -0.3, and -0.4 m^2/d (i.e., a constant-flux inland boundary condition). As shown in Figure 5a, this range of tan (β) leads to the value of r between -2.7 and 2.7. Therefore, different equations in equation (64) apply when deriving the relationship between the inland hydraulic head and freshwater flux. When $Q_f = -0.2$ m^2/d, for example, x_t is between 233.8 and 577 m and decreases with increasingtan (β)(see Figure 5b). It is not surprising that a larger magnitude of the inland freshwater flux results in a smaller x_t but a larger H_L (see Figures 5b and 5c).

Figure 6 shows the values of r, interface tip locations, and inland freshwater fluxes for different tan (β) with $H_L = 41.5$, 42, and 42.5 m (i.e., a constant-head inland boundary condition). When $H_L = 41.5$ m, x_t is between 281.2 and 635.6 m and decreases with increasing tan (β)(see Figure 6b). The effect of tan (β) on x_t is less significant for a larger H_L. For example, when $H_L = 42.5$ m, x_t decreases by only about 15 m as tan (β) increases from -0.02 to 0.02. On the other hand, a larger H_L results in a larger Q_f (see Figure 6c). For the demonstration purpose, the saltwater interfaces in a sloping unconfined aquifer (tan(β) $= \pm 0.02$) with $H_L = 41.5$, 42, and 42.5 m are shown in Figure 7. It is clearly shown that tan(β) controls the location of the interface tip.

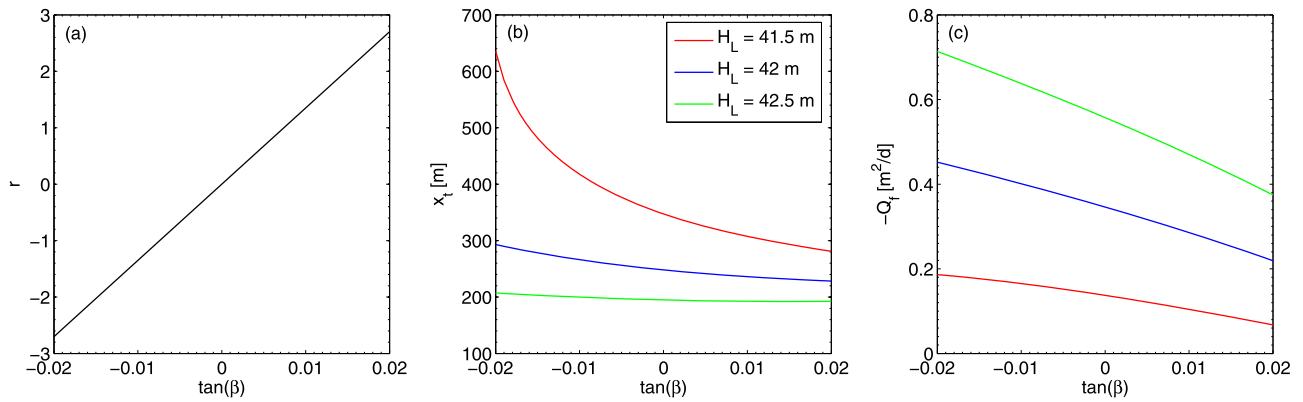

Figure 6. Values of (a) r, (b) x_t, and (c) $-Q_f$ for different values of tan(β) and $H_L = 41.5$, 42, and 42.5 m.

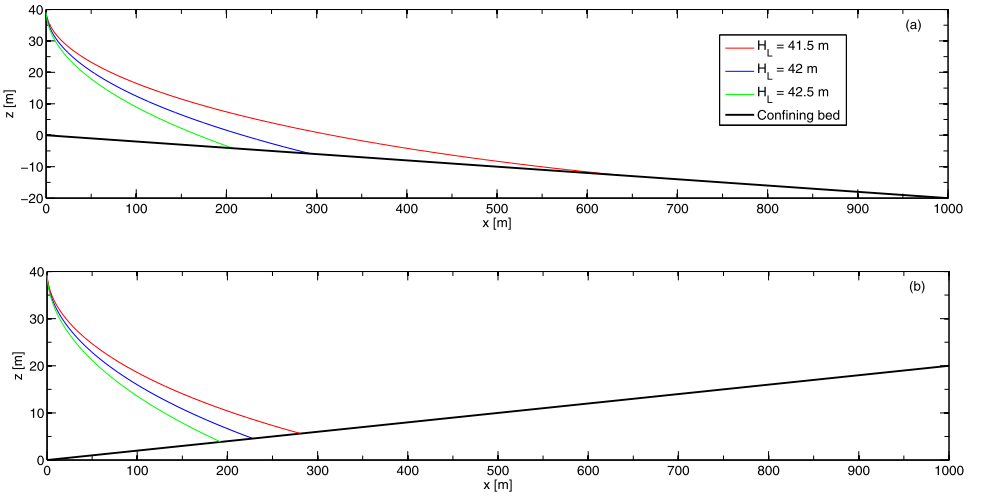

Figure 7. Saltwater interfaces in a sloping unconfined aquifer with $H_L = 41.5$, 42, and 42.5 m: (a) $\tan(\beta) = -0.02$ and (b) $\tan(\beta) = 0.02$.

5. Comparison Between Analytical and Numerical Solutions

To validate analytical solutions developed, we compare them with numerical solutions based on SEAWAT [*Langevin and Guo*, 2006]. The length of the grid in the numerical model is uniformly set to 1 m, while the height of the grid is varied between 0.25 and 0.3 m to produce a sloping aquifer. For all cases, the longitudinal dispersivity and transverse dispersivity are assumed to be 1 and 0.1 m, respectively. The parameter values for confined aquifers are assumed exactly the same as those in equation (67), while for unconfined aquifers parameter values in equation (68) together with $Q_f = -0.25$ m^2/d are employed. Moreover, $\tan(\beta_1)=0.01$ and $\tan(\beta_2) = -0.1$ and 0.1 are assumed for two confined aquifers, while $\tan(\beta) = -0.1$ and 0.1 is taken for two unconfined aquifers.

Figure 8 shows the comparison between analytical and numerical solutions for both confined and unconfined aquifer cases. Clearly, the corrected analytical solutions match well with 50% seawater concentration contourlines for all cases. By contrast, a significant difference between the two types of solutions exists if the dispersive mixing effects are not considered in the analytical solutions. In particular, this difference is more pronounced in cases with a negative slope of the bottom confining layer. The benefit of using analytical solutions is obvious in terms of computation time. The time taken for a typical case using variable-

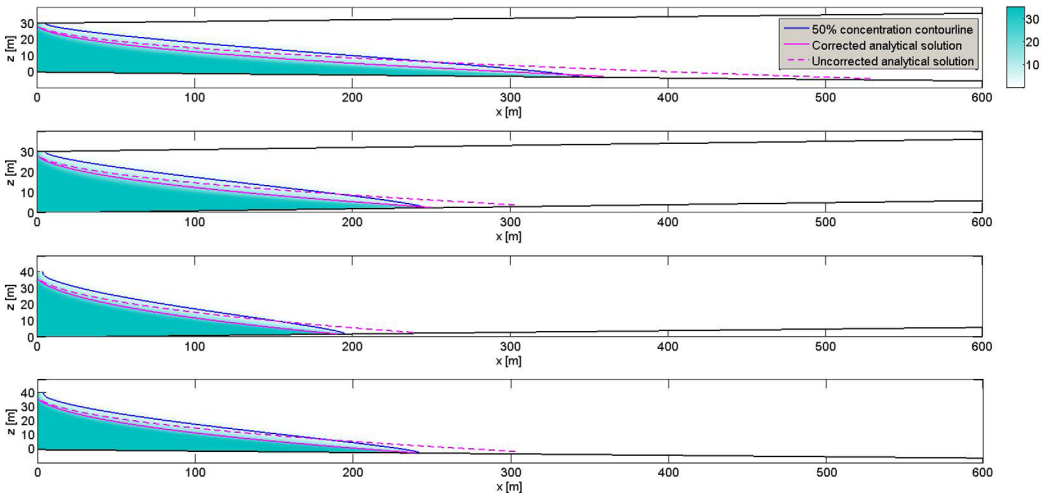

Figure 8. Comparison between analytical solutions and numerical solutions: (a) confined aquifer ($\tan(\beta_1)=0.01$ and $\tan(\beta_1)=-0.01$), (b) confined aquifer ($\tan(\beta_1)=0.01$ and $\tan(\beta_1)=0.01$), (c) unconfined aquifer ($\tan(\beta)=0.01$), and (d) unconfined aquifer ($\tan(\beta)=-0.01$).

density flow numerical modelling is in order of hours, while less than 1 min is needed by adopting developed analytical solutions.

6. Conclusions

We have derived steady state sharp-interface analytical solutions for seawater intrusion in sloping confined and unconfined aquifers. The method is based on the Dupuit-Forchheimer approximation and sharp-interface assumption. Analytical solutions for the constant-flux inland boundary condition are developed by solving the discharge equation for the interface zone with the continuity conditions of head and flux applied at the interface between the freshwater zone and the interface zone. Analytical solutions for the constant-head inland boundary condition are developed by deriving the relationship between the inland freshwater flux and hydraulic head and combining this relationship with analytical solutions of the constant-flux inland boundary condition. Based on the developed solutions, we have the following findings:

1. For confined aquifers with a constant-flux inland boundary condition, the solutions of the saltwater interface are different for $\beta_1=0$ and $\beta_1 \neq 0$, but not a function of β_2. Given a value ofβ_1, β_2 determines the location of the interface tip. The relationship between the inland hydraulic head and freshwater flux depends on whether β_1 is equal to β_2 or not.
2. For unconfined aquifers with a constant-flux inland boundary condition, the solution of saltwater interface is independent of β, while β only controls the location of the interface tip. The relationship between the inland hydraulic head and freshwater flux relies on whether $|r|=|\tan(\beta)|\sqrt{\frac{K}{N}}$ is larger, equal to, or less than 2.

In summary, it can be inferred that the interface tip location can be determined for the aquifer with a known inland freshwater flux and an arbitrary geometrical bottom confining boundary. The hydraulic head at the interface is physically controlled by the coastal boundary, so the shape of the bed below the interface is irrelevant to the interface position. Moreover, a good agreement between analytical solutions with a correction factor and numerical solutions of a variable-density flow model is obtained. Analytical solutions developed in this study are expected to provide a powerful tool for assessment of seawater intrusion changes in sloping coastal aquifers in response to various hydrological stresses such as variations in infiltration or/and sea level rise.

Appendix A: Derivation of Equation (2)

The Ghyben-Herzberg relation gives:

$$\frac{1}{\alpha}=\frac{\varphi-H_s}{h_s} \tag{A1}$$

Thus, h_s can be expressed as:

$$h_s=\alpha(\varphi-H_s) \tag{A2}$$

The vertical thickness of the freshwater lens (h) in the interface zone is determined by:

$$h=h_s-[H_s-H-x\tan(\beta_1)] \tag{A3}$$

Combining equations (A2) and (A3) yields:

$$h=\alpha(\varphi-H_s)-[H_s-H-x\tan(\beta_1)] \tag{A4}$$

Acknowledgments
This work was supported by the Fundamental Research Funds for the Central Universities (2015B28714) and National Key Research Project (2016YFC0402800). The authors would like to thank Antonis D. Koussis, anonymous reviewers, and editors for their valuable comments and suggestions. The data used in this paper can be obtained upon request from the corresponding author.

References

Abarca, E., J. Carrera, C. I. Voss, and X. Sánchez-Vila (2002), Effect of aquifer bottom morphology on seawater intrusion, in *17th Salt Water Intrusion Meeting (SWIM)*, Delft.

Akylas, E., A. D. Koussis, and A. N. Yannacopoulos (2006), Analytical solution of transient flow in a sloping soil layer with recharge, *J. Hydrol. Sci.*, *51*(4), 626–641.

Ataie-Ashtiani, B., R. E. Volker, and D. A. Lockington (1999), Tidal effects on sea water intrusion in unconfined aquifers, *J. Hydrol.*, *216*(1-2), 17–31.

Badon Ghyben, W., and J. Drabbe (1888), Nota in verband met de voorgenomen putboring nabij Amsterdam, in *Tijdschr. Kon. Inst. Ing.*, pp. 8–22, Gravenhage, Netherlands.

Bakker, M., and F. Schaars (2013), Modeling steady sea water intrusion with single-density groundwater codes, *Groundwater*, *51*(1), 135–144.
Bakker, M. (2014), Exact versus Dupuit interface flow in anisotropic coastal aquifers, *Water Resour. Res.*, *50*, 7973–7983, doi:10.1002/2014WR016096.
Basha, H. A., and S. F. Maalouf (2005), Theoretical and conceptual models of subsurface hillslope flows, *Water Resour. Res.*, *41*, W07018, doi:10.1029/2004WR003769.
Bear, J. (1972), *Dynamics of Fluids in Porous Media*, Elsevier, Amsterdam, Netherlands.
Beebe, C., G. Ferguson, T. Gleeson, L. K. Morgan, and A. D. Werner (2016), Application of an analytical solution as a screening tool for sea water intrusion, *Groundwater*, doi:10.1111/gwat.1241, in press.
Chapuis, R. P. (2002), Solution analytique de l'écoulement en régime permanent dans un aquifère incliné á nappe libre, et comparaison de cette solution avec des solutions numériques plus complètes, *Rapport Tech. EPM-RT-02-03*, août 2002, École Polytech., Montréal. [Available at http://www.polymtl.ca/biblio/epmrt/rapports/rt2003-03.pdf.]
Chapuis, R. P. (2011), Steady state groundwater seepage in sloping unconfined aquifers, *Bull. Eng. Geol. Environ.*, *70*, 89–99.
Cheng, A. H.-D., D. Halhal, A. Naji, and D. Ouazar (2000), Pumping optimization in saltwater-intruded coastal aquifers, *Water Resour. Res.*, *36*(8), 2155–2165.
Dupuit, J. (1863), *Études Théoriques et Pratiques sur le Mouvement des Eaux dans les Canaux Decouverts et à Travers les Terrains Perméables*, 2íeme ed., Dunod, Paris.
Ferguson, G., and T. Gleeson (2012), Vulnerability of coastal aquifers to groundwater use and climate change, *Nat. Clim. Change*, *2*(5), 342–345.
Forchheimer, P. (1886), Ueber die Ergiebigkeit von Brunnen-Anlagen und Sickerschlitzen, *Z. Architkt. Ing. Verlag*, *32*, 539–563.
Henderson, F.M., and R.A. Wooding (1964), Overland flow and groundwater flow from a steady rainfall of finite duration, *J. Geophys. Res.*, *69*(8), 1531–1540.
Herzberg, A. (1901), Die Wasserversorgung einiger Nordseebäder, *J. Gasbeleucht. Wasserversorg.*, *44*, 815–819, 842–844.
Huang, C.-S., S.-Y. Yang, and H.-D. Yeh (2014), Groundwater flow to a pumping well in a sloping fault zone unconfined aquifer, *Water Resour. Res.*, *50*, 4079–4094, doi:10.1002/2013WR014212.
Kacimov, A. R. (2001), Analytical solution to a sharp interface problem in a vortex-generate flow, *Water Resour. Res.*, *37*(12), 3387–3391.
Kacimov, A. R., and Y. V. Obnosov (2001), Analytical solution for a sharp interface problem in seawater intrusion into a coastal aquifer, *Proc. R. Soc. London Ser. A*, *457*, 3023–3038.
Koussis, A. D., et al. (2010), Cost-efficient management of coastal aquifers via recharge with treated wastewater and desalination of brackish groundwater: Application to the Akrotiri Basin and Aquifer, Cyprus. *Hydrol. Sci. J.*, *55*(7), 1234–1245.
Koussis, A. D., K. Mazi, and G. Destouni (2012), Analytical single-potential, sharp-interface solutions for regional seawater intrusion in sloping unconfined coastal aquifers, with pumping and recharge, *J. Hydrol.*, *416–417*, 1–11.
Koussis, A.D., K. Mazi, F. Riou, and G. Destouni (2015), A correction for Dupuit-Forchheimer interface flow models of seawater intrusion in unconfined coastal aquifers, *J. Hydrol.*, *525*, 277–285.
Kuan, W. K., G. Jin, P. Xin, C. Robinson, B. Gibbes, and L. Li (2012), Tidal influence on seawater intrusion in unconfined coastal aquifers, *Water Resour. Res.*, *48*, W02502, doi:10.1029/2011WR010678.
Langevin, C. D., and W. Guo (2006), MODFLOW/MT3DMS-based simulation of variable-density ground water f low and transport, *Groundwater*, *44*, 339–351, doi:10.1111/j.1745-6584.2005.00156.x.
Loáiciga, H. A. (2005), Steady state phreatic surfaces in sloping aquifers, *Water Resour. Res.*, *41*, W08402, doi:10.1029/2004WR003861.
Lu, C., and J. Luo (2010), Dynamics of freshwater-seawater mixing zone development in dual-domain formations, *Water Resour. Res.*, *46*, W11601, doi:10.1029/2010WR009344.
Lu, C., and J. Luo (2014), Groundwater pumping in head-controlled coastal systems: The role of lateral boundaries in quantifying the interface toe location and maximum pumping rate, *J. Hydrol.*, *512*, 147–156.
Lu, C., and A. D. Werner (2013), Timescales of seawater intrusion and retreat, *Adv. Water Resour.*, *59*, 39–51.
Lu, C., P. K. Kitanidis, and J. Luo (2009), Effects of kinetic mass transfer and transient flow conditions on widening mixing zones in coastal aquifers, *Water Resour. Res.*, *45*, W12402, doi:10.1029/2008WR007643.
Lu, C., Y. Chen, and J. Luo (2012), Boundary condition effects on maximum groundwater withdrawal in coastal aquifers, *Groundwater*, *50*(3), 386–393.
Lu, C., A. D. Werner, and C. T. Simmons (2013a), Threats to coastal aquifers, *Nat. Clim. Change*, *3*(7), 605.
Lu, C., Y. Chen, C. Zhang, and J. Luo (2013b), Steady-state freshwater-seawater mixing zone in stratified coastal aquifers, *J. Hydrol.*, *505*, 24–34.
Lu, C., A. D. Werner, C. T. Simmons, N. I. Robinson, and J. Luo (2013c), Maximizing net extraction using an injection-extraction well pair in a coastal aquifer, *Groundwater*, *51*(2), 219–228.
Lu, C., P. Xin, L. Li, and J. Luo (2015), Seawater intrusion in response to sea-level rise in a coastal aquifer with a general-head inland boundary, *J. Hydrol.*, *522*, 135–140.
Mantoglou, A. (2003), Pumping management of coastal aquifers using analytical models of saltwater intrusion, *Water Resour. Res.*, *39*(12), 1335, doi:10.1029/2002WR001891.
Mazi, K., A. D. Koussis, and G. Destouni (2013), Tipping points for seawater intrusion in coastal aquifers under rising sea level, *Environ. Res. Lett.*, *8*, 014001.
McEnroe, B. M. (1993), Maximum saturated depth over landfill liner, *J. Environ. Eng.*, *119*(2), 262–270.
Park, N., L. Cui, and L. Shi (2009), Analytical design curves to maximize pumping or minimize injection in coastal aquifers, *Groundwater*, *47*(6), 797–805.
Pool, M., and J. Carrera (2011), A correction factor to account for mixing in Ghyben-Herzberg and critical pumping rate approximations of seawater intrusion in coastal aquifers, *Water Resour. Res.*, *47*, W05506, doi:10.1029/2010WR010256.
Post, V. and E. Abarca (2010), Preface: Saltwater and freshwater interactions in coastal aquifers, *Hydrogeol. J.*, *18*, 1–4.
Qahman, K. A., and Y. Zhou (2001), Monitoring of seawater intrusion in the Gaza Strip, Palestine, in First International Conference on Saltwater Intrusion and Coastal Aquifers Monitoring, Modeling, and Management, Essaouira, Morocco, 23–25 Apr.
Sherif, M. M., and V. P. Singh (1999), Effect of climate change on sea water intrusion in coastal aquifers, *Hydrol. Process.*, *13*(8), 1277–1287.
Strack, O. D. L. (1976), A single-potential solution for regional interface problems in coastal aquifers, *Water Resour. Res.*, *12*(6), 1165–1174.
Strack, O. D. L. (1989), *Groundwater Mechanics*, Prentice Hall, Englewood Cliffs, N. J.

Strack, O. D. L., and B. K. Ausk (2015), A formulation for vertically integrated groundwater flow in a stratified coastal aquifer, *Water Resour. Res.*, *51*, 6756–6775, doi:10.1002/2015WR016887.

Verhoest, N. F. C., and P. A. Troch (2000), Some analytical solutions of the linearized Boussinesq equation with recharge for a sloping aquifer, *Water Resour. Res.*, *36*(3), 793–800.

Werner, A. D., and C. T. Simmons (2009), Impact of sea-level rise on sea water intrusion in coastal aquifers, *Groundwater*, *47*(2), 197–204.

Werner, A. D., M. Bakker, V. Post, A. Vandenbohede, C. Lu, B. Ataie-Ashtiani, C. Simmons, and D. A. Barry (2013), Seawater intrusion processes, investigation and management: Recent advances and future challenges, *Adv. Water Resour.*, *51*, 3–26.

Xin, P., C. Robinson, L. Li, D. A. Barry, and R. Bakhtyar (2010), Effects of wave forcing on a subterranean estuary, *Water Resour. Res.*, *46*, W12505, doi:10.1029/2010WR009632.